PHILOSOPHICAL TRANSACTIONS OF THE ROYAL SOCIETY A MATHEMATICAL, PHYSICAL & ENGINEERING SCIENCES

Exploration of Radiative Properties of Very Excited Atoms

S. Haroche, P. Goy, J. M. Raimond, C. Fabre and M. Gross

Phil. Trans. R. Soc. Lond. A 1982 **307**, 659-672
doi: 10.1098/rsta.1982.0137

Phil. Trans. R. Soc. Lond. A **307**, 659–672 (1982)
Printed in Great Britain

Exploration of radiative properties of very excited atoms

By S. Haroche, P. Goy, J. M. Raimond, C. Fabre and M. Gross
Laboratoire de Physique de l'École Normale Supérieure, 24 *rue Lhomond*,
75321 *Paris cedex* 05, *France*

Various experiments involving very excited atoms and millimetre-wave photons are described, including high-resolution spectroscopy of Rydberg transitions, Rabi nutation and transient maser action between Rydberg levels.

The large number of extremely narrow Rydberg spectral lines observed throughout the millimetre-wave spectrum provide a very good 'calibration' of the scale of Rydberg levels of Na and Cs near the ionization limit, which could be used for the realization of precise infrared frequency markers.

The observation of Rabi nutation and maser signals involving an unusually small absolute number of atoms and photons reveals the very great strength of the Rydberg atom to radiation coupling and is a clear indication that these atoms could be used as extremely sensitive millimetre-wave detectors. At a more fundamental level, the study of transient Rydberg masers provides a test of superradiance theory. Extrapolation of these maser experiments to the investigation of a situation where a single atom would exchange a single millimetre-wave photon with a resonant cavity is considered.

1. Introduction

Rydberg atoms, prepared by exciting a valence electron to a state very close to the atomic ionization limit, are extremely sensitive to millimetre-wave radiation. These atoms are also very stable against spontaneous radiative decay, resulting in unusually narrow atomic spectral lines. In this paper, various aspects of the peculiar radiative properties of these atoms will be described. In the field of spectroscopy, the resonant absorption of millimetre-wave photons – in single or multiphoton processes – has allowed us to achieve a very precise mapping of the energy levels of alkali atoms near the ionization limit, with a precise determination of quantum defects, fine and hyperfine structures. Possible application of these experiments to metrology will be discussed. Another very interesting aspect of the Rydberg atoms' radiative properties concerns the coherent interaction of these atoms with resonant cavities. Owing to the very large electric dipole moments in Rydberg states, the atom–radiation coupling is extremely strong, resulting in the possibility of observing Rabi nutation signals induced by small numbers of photons in the cavity and in an unusually large radiative damping of the atomic system interacting with the cavity walls. If the atoms are prepared in the upper level of an atomic transition resonant with a cavity mode, a short maser pulse is emitted in a process quite analogous to superradiance. This Rydberg maser effect has an extremely low inversion threshold, about a hundred atoms being, at the present stage of the experiment, enough to observe maser emission. Reduction of this atom number to a few – ultimately to a single unit – seems to be an accessible goal and would allow us to check the laws of electrodynamics on an unfamiliar scale. All these experiments clearly indicate that Rydberg atoms could serve as very good detectors and amplifiers of millimetre-wave radiation, in a frequency range where efficient receivers are in high demand. Some applications of Rydberg atoms to detection technology will be considered in the conclusion of this review.

2. General scheme of experiments

The general set-up developed for most of the experiments described in this paper is shown in figure 1.

2.1. *Rydberg atom preparation*

The Rydberg atoms are produced by pulsed laser excitation of an atomic beam of alkali atoms (Na or Cs) (Fabre *et al.* 1978, 1980; Goy *et al.* 1982). An nS or an nD level (n is the principal quantum number of the order of 20 to 40) is prepared by absorption of two successive optical photons (transitions 3S → 3P → nS or nD for Na and 6S → 6P → nS or nD for Cs). The excitation

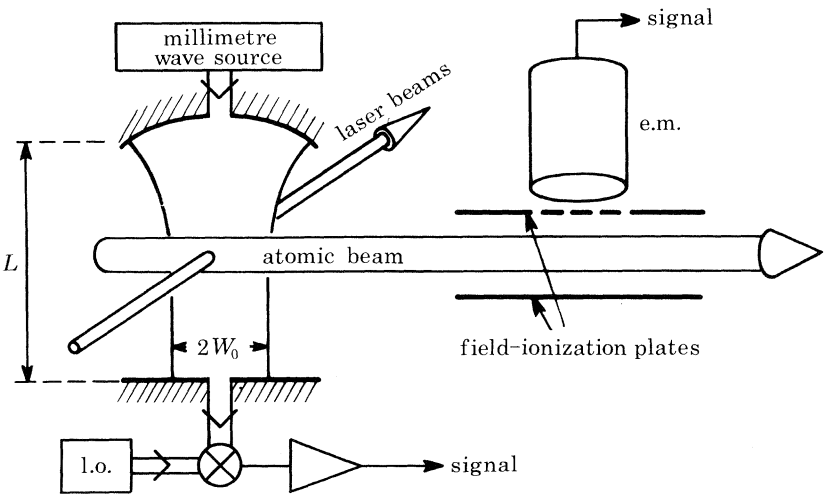

Figure 1. Experimental arrangement for Rydberg atom–radiation interaction experiments.

is performed with the help of two pulsed dye lasers pumped by the same N_2 or YAG laser. It allows us to prepare within a couple of nanoseconds a number of atoms, from 1 to about 10^6 at a pulse repetition rate of 10 s^{-1}. After they have been excited, the Rydberg atoms drift along the atomic beam along a path of several centimetres before they spontaneously decay towards lower levels (typical spontaneous emission time for a $n \approx 30$ level is 20 μs).

2.2. *Interaction with millimetre-wave radiation*

In most experiments, the atoms interact with the millimetre-wave radiation inside a cavity of the open Fabry–Perot type, whose axis is perpendicular to the atomic beam direction and whose frequency can be tuned to the atomic transition between Rydberg levels by intermirror length adjustments (typical cavity length $L \approx 1$ cm). The cavity sustains a Gaussian mode having a waist W_0 (typical value of W_0 is a few millimetres), the volume $v = LW_0^2$ of the mode in the cavity being typically of the order of 0.1 cm^3. The cavity Q factor is of the order of 10^4. For spectroscopic experiments requiring a frequency-tunable external radiation, the cavity is coupled through a waveguide to a millimetre-wave source (carcinotron or frequency-multiplied X-band klystron), frequency-locked to a quartz oscillator (Goy *et al.* 1982).

2.3. *Millimetre-wave field detection*

The radiation, coming out from the cavity through a second wave guide, can be detected by a Schottky diode heterodyne receiver, primarily designed for radioastronomy applications

(Moi *et al.* 1980). This diode beats the millimetre-wave signal to be measured against a local oscillator reference wave, the beat note (in the hundred megahertz range) being amplified and displayed on a fast scope.

2.4. *Atomic detection*

After having crossed the cavity, the atoms drift through the plates of a condenser to which a time-varying electric field is applied. The purpose of this field is to ionize the atoms, the resulting electrons being collected and counted by an electron multiplier. We make use of the fact that

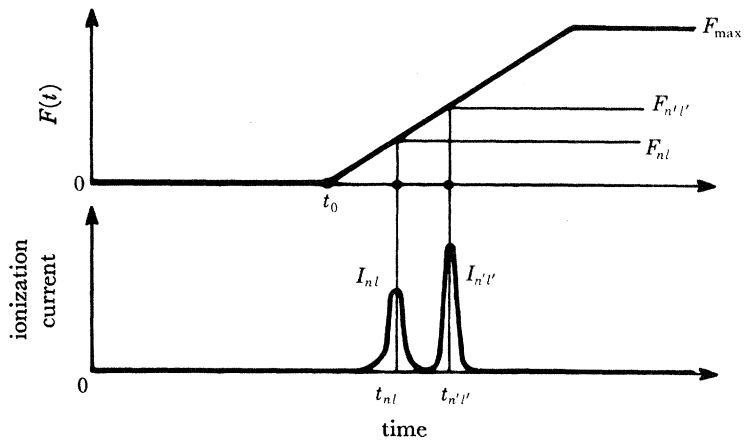

FIGURE 2. Time sequence of events for Rydberg state-selective field ionization detection ($F(t)$ is a time-varying electric field).

the minimum electric field required to ionize an atom increases with its binding energy, which provides an easy way of discriminating between Rydberg levels corresponding to different n values (Fabre *et al.* 1978). The timing of a typical experiment is sketched in figure 2: at time $t = 0$, the lasers prepare the Rydberg atoms in the cavity in an initial level $|nl\rangle$ (l is the angular momentum quantum number equal to 0 for an S state, to 2 for a D state). The atoms then interact with the radiation, which induces transitions towards $|n'l'\rangle$ levels. They drift out of the cavity and at a time $t_0 \approx 20$ μs arrive in the middle of the condenser. At this time, a ramp of electric field is started (ramp duration of the order of 1 μs). This ramp reaches at different times t_{nl} and $t_{n'l'}$ the threshold fields for ionizing levels $|nl\rangle$, $|n'l'\rangle$... so that time-resolved electron peaks I_{nl}, $I_{n'l'}$ are detected at these times by the electron multiplier. The number of charges in each electron peak is directly related – knowing the gain of the detection system – to the population of the corresponding Rydberg level at time t_0. Any change of these populations due to a radiatively induced transition between $|nl\rangle$ and $|n'l'\rangle$ is revealed by a modification of the ratio $I_{n'l'}/I_{nl}$ and can be easily detected. Signal processing (calibration of electron peak and ratio computation) is performed by a computer interfaced to a fast transient digitizer scope connected to the electron multiplier output.

The set-up just described is the most general and versatile one used for our Rydberg-radiation experiments. Usually, as shown below, only part of it is actually needed in a specific experiment. For example, some spectroscopic measurements do not require a resonant cavity and can be performed without it. The cavity region in figure 1 is then replaced by an open interaction space coupled to the microwave source by a horn. Only some specific experiments

(Rydberg masers) make use of the sophisticated heterodyne receiver described in § 2.2. For all other experiments, this detector is disconnected and the detection relies entirely on the more versatile Rydberg atom detector. For more technical details concerning any of the experiments discussed below, the reader can find information in the references given in the text.

3. Outline of the millimetre-wave–Rydberg-atom spectroscopy experiments

Using the set-up described in the previous section, we have carried out an extensive study of $nl \rightarrow n'l'$ transitions in Na and Cs with $n \approx 20$–45, $l = 0$ to 3, $n' - n = 0, 1, 2$; $l' - l = 0$ or 1. The transition frequencies ranged from 50 to 450 GHz (Fabre *et al.* 1978, 1980; Goy *et al.* 1982). Figure 3 shows a section of the energy spectrum of caesium near the ionization limit on which the transitions we have studied are represented by arrows.

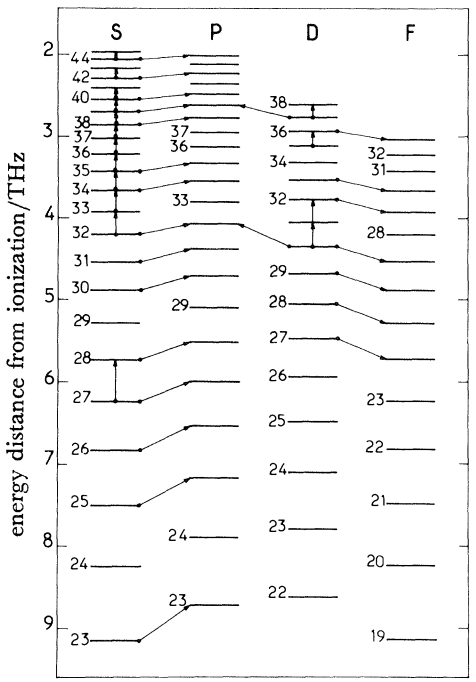

Figure 3. Section of caesium energy levels near the ionization limit with observed millimetre wave transitions marked by arrows.

To record the signals, we measured the ratio $I_{n'l'}/I_{nl}$ as the frequency of the millimetre wave (delivered by a carcinotron or a frequency-multiplied klystron) was swept across resonance. Owing to the extremely large value of the electric dipole matrix elements between Rydberg states ($d = \langle nl|qr|n'l'\rangle$ is of the order of 500 atomic units for $n = n' \approx 30$), exceedingly low amounts of millimetre wave (in the nanowatt to picowatt range) were enough to induce the transitions. We have detected both single-photon and two-photon transitions. Figure 4 presents as an example a two-photon line observed in Na (39S $\rightarrow$ 40S transition at $2\nu = 118.52$ GHz). Since the atoms absorb the two photons in the standing-wave pattern of the resonant cavity, the Doppler effect is cancelled (Grynberg & Cagnac 1977) and the line is very narrow (about 10 kHz), reflecting in fact the limitation due to finite transit time in the cavity waist. Figure 5

PHILOSOPHICAL TRANSACTIONS OF THE ROYAL SOCIETY A MATHEMATICAL, PHYSICAL & ENGINEERING SCIENCES

shows an example of a single-photon line: ($28S_{\frac{1}{2}} \rightarrow 28P_{\frac{1}{2}}$ transition in Cs at $\nu = 213.022$ GHz). In this recording, there was no resonant cavity around the atoms and the interaction with radiation was performed in a free-running wave configuration. The line widths (in the 600 kHz range) are much larger than in figure 4, but they are still narrow enough to reveal a hyperfine structure due to the interaction of the Rydberg electron with the nuclear spin (hyperfine splitting between the $F = 4$ and $F' = 3$ sublevels in the $28S_{\frac{1}{2}}$ and $28P_{\frac{1}{2}}$ states).

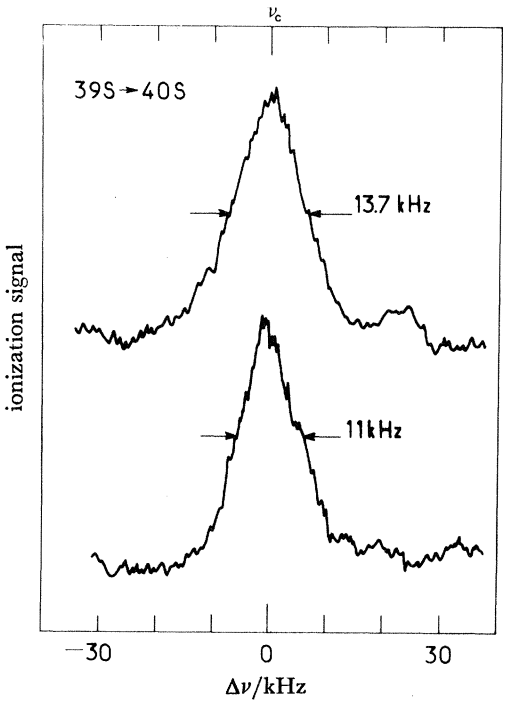

FIGURE 4. Two-photon Doppler-free 39S → 40S resonance in Na at $2\nu = 118.52$ GHz (the two traces correspond to different transit times in the cavity waist).

For an understanding of the systematics of the observed spectra, it is appropriate to briefly recall here the basic features of Rydberg-level spectroscopy in the alkalis.

To 'zero-order approximation', the valence electron in a Rydberg atom interacts with a point-like charge located at the nucleus and its energy is given by the hydrogen-like Rydberg formula:

$$E_n = -R/n^2, \tag{1}$$

where $R = 3.289\,828 \times 10^9$ MHz is the Rydberg constant.

In fact, for an $|nlJ\rangle$ level in an alkali atom (J is the total electronic angular momentum equal to $l \pm \frac{1}{2}$), n has to be replaced by $n^* = n - \delta_{nlJ}$ where δ_{nlJ} is the so-called 'quantum defect' describing the perturbation of the atomic core on the valence electron. One must write instead of (1):

$$E_{nlJ} = -R/(n-\delta_{nlJ})^2. \tag{2}$$

δ_{nlJ} depends of course upon the species (it increases with the atomic number of the alkali) and upon the angular momentum l of the level (it decreases with increasing l values corresponding to fewer and fewer 'core-penetrating' orbitals). For precise measurements, we must also take

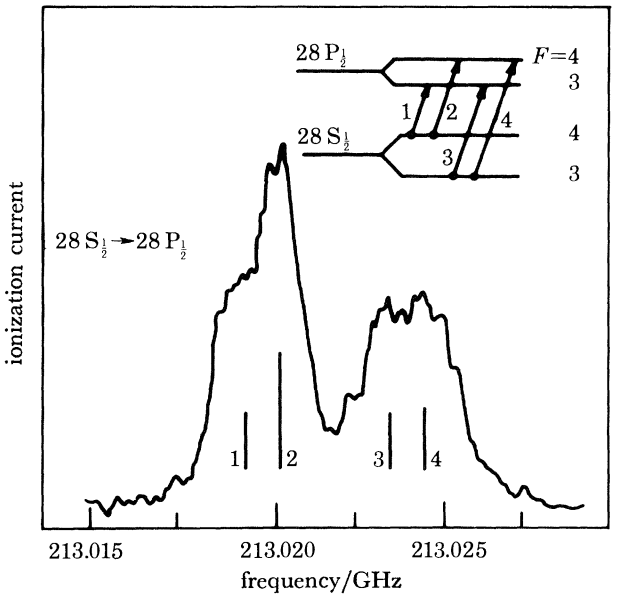

FIGURE 5. Single-photon 28S → 28P½ transition in caesium exhibiting the hyperfine structures of 28S½ and 28P½ levels.

into account a slight dependence of δ_{nlJ} upon J and upon n. The latter is conveniently expressed as an expansion in inverse power of the binding energy (Ritz formula):

$$\delta_{nlJ} = \delta_{lJ}(+\infty) + a_{lJ}/(n^*)^2 + \ldots, \tag{3}$$

where δ_{lJ}, a_{lJ} are a set of constants. From (2) and (3), it is possible to express with very good accuracy, and with the help of a small number of parameters, the frequency of any transition between Rydberg levels as:

$$\nu_{nlJ\to n'l'J'} = \frac{R}{n}\left[\frac{1}{\{n^* - \delta_{lJ} - a_{lJ}(n^*)^{-2} - \ldots\}^2} - \frac{1}{\{n'^* - \delta_{l'J'} - a_{l'J'}(n'^*)^{-2} - \ldots\}^2}\right]. \tag{4}$$

The dependence on J in (4) accounts for the fine structure of the transitions connecting levels with l or l' different from zero. For very precise measurements, one must add to formula (4) a very small correction accounting for the hyperfine interaction (see above).

Measurements made on more than 100 lines in Na and Cs have allowed us to determine with precision the constants δ_{lJ} and a_{lJ} in (4) (Fabre *et al.* 1980; Goy *et al.* 1982). In turn, these figures substituted into (4) allow us to predict with an accuracy better than 1 MHz the position of any previously unmeasured line (we have verified this point by using this equation to preset the millimetre-wave source frequency on transitions not yet investigated). We can also use this formula to predict the frequency of much higher-frequency lines corresponding to the $\Delta n = 10$ to 20 transitions, connecting 'moderately excited' Rydberg levels, with $n \approx 15$, to highly excited states ($n \approx 35$).

These lines fall in the middle infrared range ($\lambda \approx 20$ to 50 μm). (For deeper transitions with $n < 15$, we would need in (4) higher-order coefficients not precisely determined by our measurements in Rydberg levels.) As a result, our spectroscopy measurements provide a direct link between millimetre-wave and infrared frequencies. We have calibrated with millimetre waves the small $\Delta n = 1$ and $\Delta n = 2$ steps in the unevenly spaced scale of Rydberg levels and we could

now – using (4) – make large jumps in this scale to calibrate the frequency of lasers inducing one-step infrared transitions between the levels. As the frequency of our millimetre-wave sources is directly calibrated against the caesium atomic clock, this would constitute a very simple frequency marker for infrared frequencies. The expected accuracy in frequency determination would be 10^{-7} to 10^{-8}, much lower than obtained by heterodyne frequency mixing and counting (Evenson *et al.* 1975), but certainly much easier to achieve when ultra-high precision is not required.

Let us also mention that similar millimetre-wave experiments performed in hydrogen and deuterium would provide an alternative way for measuring the Rydberg constant (the quantum defects are then obviously zero), which so far has only been determined in wavelength and not in frequency units.

4. Rabi nutation and collective radiative damping of Rydberg atoms in a resonant cavity

We describe in this section an interesting variant of the spectroscopic experiments, revealing in a spectacular way the extreme sensitivity of Rydberg atoms to millimetre-wave fields and the strength of their radiative coupling to a resonant electromagnetic cavity.

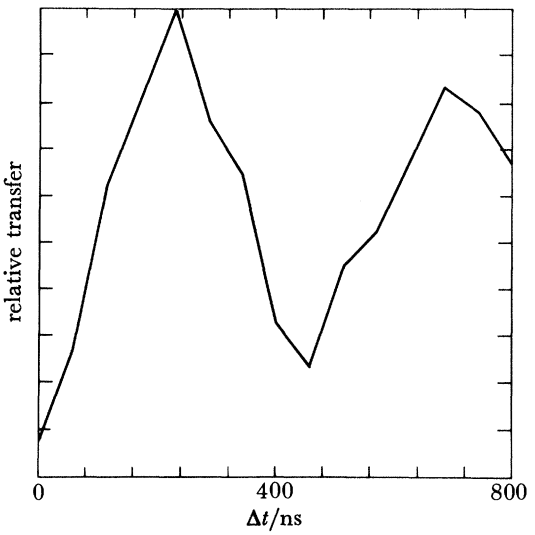

Figure 6. Rabi nutation signal corresponding to the 30S → 30P transition in Na. The millimetre field amplitude is $\mathscr{E}_1 \approx 4 \times 10^{-3}$ V cm^{-1}, corresponding to only 2000 photons stored in the cavity. The atom number N is 300.

4.1. *Rabi nutation in Rydberg levels*

Instead of sweeping the millimetre-wave frequency as in the experiments described in the previous section, it is now kept fixed at resonance and the atom–millimetre-wave interaction time Δt is varied. The atoms are interacting with the field inside the resonant cavity. Figure 6 shows as a typical example the ratio of the population of the 30P to 30S states of Na as a function of Δt, following the excitation of $N \approx 300$ Rydberg atoms at time $t = 0$ in the *lower* 30S state of the transition. One observes a strong modulation of the transfer towards the 30P state, the classical Rabi nutation signal, whose frequency

$$\nu_1 = \mathrm{d}\mathscr{E}_1/h \qquad (5)$$

is (in units of h) equal to the product of the millimetre-wave field amplitude in the cavity, $\mathscr{E}_1$, by the electric dipole matrix element of the transition ($d = 425$ atomic units). Owing to the large d value, a small field $\mathscr{E}_1$ of 4×10^{-3} V cm^{-1}, corresponding to only 2×10^3 millimetre-wave photons stored in the $v \approx 0.1$ cm^3 volume of the cavity mode is enough to produce a 2.2 MHz Rabi nutation frequency! Usually, similar Rabi nutation signals are obtained – on ordinary atoms with $d \approx 1$ atomic unit – with fields containing thousands of millions of photons! This kind of experiment can be used either to perform an absolute calibration of extremely weak monochromatic fields in the millimetre-wave domain or, if this field is known from calibration of the source and attenuators, it provides an absolute measurement of electric dipoles in Rydberg states, which amounts to a measurement of the sizes of these large atoms.

It is interesting, in view of the discussion to follow in § 5, to describe in more detail the way in which the atom–radiation interaction time Δt is varied in this experiment. At a time Δt after the laser excitation, and small enough so that the atoms are still in the cavity ($\Delta t \ll t_0$), a small d.c. voltage is applied on an electrode (not represented in figure 1) very close to the cavity (but outside its mode geometry so that it does not spoil its Q). This voltage induces a small inhomogeneous d.c. field inside the cavity, which, through Stark effect, shifts the Rydberg levels out of resonance. Thus the interaction between the atom and the field is suddenly interrupted after time Δt. The population of the levels coupled by the millimetre-wave transition are 'frozen' from that time on and the Rydberg atom detector measures at time t_0 the transfer that had been achieved after time Δt. By resuming the same experiment with increasing delays Δt, one reconstructs the Rabi nutation curve.

4.2. *Radiative damping of the Rabi nutation signal*

In figure 7 we show the modifications induced in the Rabi nutation signal when the number of atoms is increased. Figure 7*a* presents a signal similar to that of figure 6, at a somewhat higher frequency $\nu_1 = 4.2$ MHz, and corresponding to a relatively small number of atoms ($N = 300$). In figure 7*b*, the number of atoms has been increased to $N = 4500$, with all the other parameters the same. One observes a washing-out of the Rabi nutation pattern, the population of the 30P state relaxing now irreversibly towards a fixed value as Δt increases. This effect is obviously related to a collective radiative damping of the Rydberg atom system in the cavity. The electric dipoles driven in phase by the small millimetre-wave field and coupled to their images in the cavity walls do indeed undergo a very strong radiative damping with a characteristic rate (Abragam 1961):

$$T_r^{-1} = 2(d^2/\hbar\epsilon_0)\,(NQ/v). \tag{6}$$

In order to observe the Rabi nutation at frequency ν_1, the condition

$$2\pi\nu_1 T_r > 1 \tag{7}$$

should be fulfilled, which basically means that the driving field $\mathscr{E}_1$ should remain larger than the self-radiated one. Replacing in (5), (6) and (7) the various parameters by their values, one finds that the nutation cannot be observed for $N \gtrsim 2000$, in fair agreement with the experimental observation. Of course, cavity-induced radiative damping effects are well known in ordinary electronic or magnetic resonance experiments (Abragam 1961). However, for ordinary electric or magnetic dipoles, effective damping in $Q \approx 10^4$ cavities requires atom numbers in

PHILOSOPHICAL TRANSACTIONS OF THE ROYAL SOCIETY A MATHEMATICAL, PHYSICAL & ENGINEERING SCIENCES

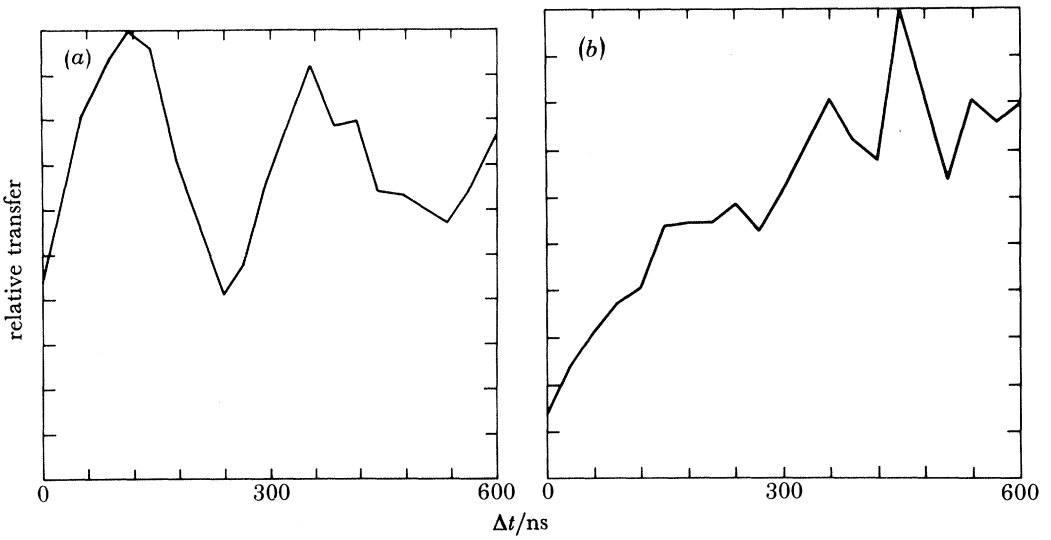

FIGURE 7. Radiative damping of the Rabi nutation signal. (*a*) Rabi nutation signal with small atom number ($N = 300$). (*b*) Signal observed in the same field with 4500 atoms: the Rabi nutation has been destroyed by radiative damping.

the range 10^9–10^{12}. In Rydberg atoms, similar effects are clearly observable in 'microscopic samples' with only a few thousand radiators.

Such collective damping effects should of course be avoided in precise spectroscopic measurements performed in cavities. To exclude unwanted collective line broadenings, the number of atoms in the Rydberg sample must be kept in these experiments in the $N \approx 100$ range.

5. RYDBERG ATOM MASERS

A resonant radiative transfer of atoms between two Rydberg levels can occur even without any externally applied millimetre-wave field: if a large enough number of atoms are prepared in the *upper* level of a transition resonant with the millimetre-wave cavity, they undergo a fast decay towards the lower level and emit a millimetre-wave radiation burst at the frequency of this transition. This is a transient maser effect that we have observed on a very large number of $\Delta n = 1$ and $\Delta n = 2$ transitions in Na and Cs (Gross *et al.* 1979; Moi *et al.* 1983).

The maser action between two Rydberg levels $|nl\rangle$ and $|n'l'\rangle$ can be simply understood within the very simple model sketched in figure 8*a*: each Rydberg atom being described as a two-level system† analogous to a spin $\frac{1}{2}$ particle, the whole atomic system made of N atoms is isomorphous to a $J = \frac{1}{2}N$ angular momentum (so-called Bloch vector), which, during the maser evolution, flips from the initial 'up' position (all atoms in the upper level) to the final 'down' position (all atoms in the lower level). Each stage of the maser evolution can be represented by the Bloch angle θ between the 'up' position and the position of the Bloch vector at that time. The evolution of the angle θ is given by (Moi *et al.* 1983)

$$\frac{\mathrm{d}^2\theta}{\mathrm{d}t^2} + \frac{1}{2T_{\mathrm{cav}}}\frac{\mathrm{d}\theta}{\mathrm{d}t} - \frac{1}{4T_{\mathrm{r}}T_{\mathrm{cav}}}\sin\theta = 0, \tag{8}$$

† One neglects all other atomic levels not connected by the maser transition. One also disregards effects due to level degeneracy. This model is shown to be exactly valid for a $n\mathrm{S}_{\frac{1}{2}} \rightarrow n\mathrm{P}_{\frac{1}{2}}$ transition (see Moi *et al.* 1983).

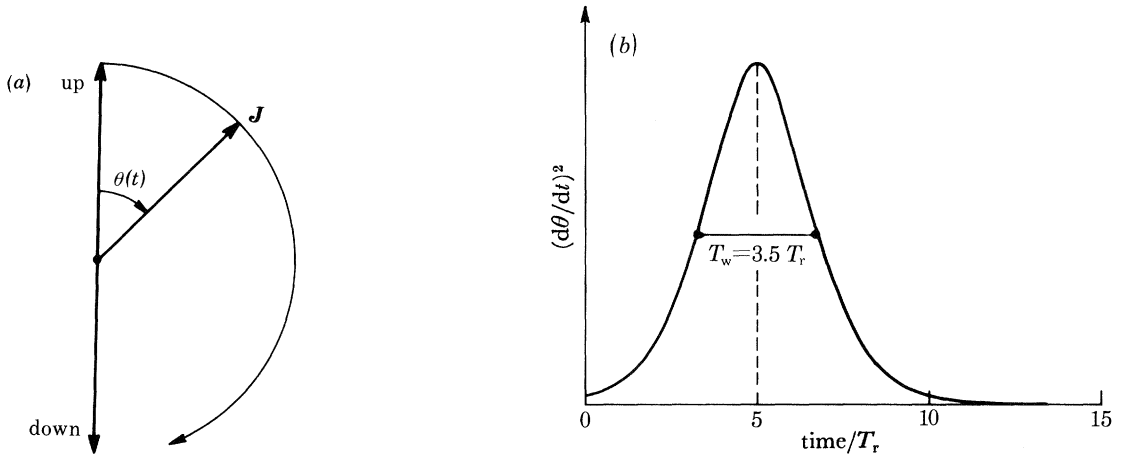

FIGURE 8. Simple Bloch-vector model of a Rydberg maser: (*a*) the atomic system polarization behaves as an angular momentum $\boldsymbol{J}$ (Bloch-vector) flipping from the initial 'up' to the final 'down' position; (*b*) time evolution of the kinetic energy of this Bloch-vector, which represents the radiated energy of the maser (case corresponding to $T_{\mathrm{cav}} \ll T_{\mathrm{r}}$).

where $T_{\mathrm{cav}} = Q/2\pi\nu$ is the characteristic cavity damping time and T_{r} is the collective atoms–cavity coupling time defined by (6). The Bloch angle thus undergoes a 'pendulum-like equation' analogous to the evolution of a particle damped by a viscous decay term $((1/2T_{\mathrm{cav}})\ (\mathrm{d}\theta/\mathrm{d}t))$ in a potential well proportional to $\cos\theta$. The electromagnetic energy radiated at time t in the cavity, W_{r}, is merely proportional to the kinetic energy of this pendulum:

$$W_{\mathrm{r}} \propto (\mathrm{d}\theta/\mathrm{d}t)^2. \tag{9}$$

At time $t = 0$, the pendulum initially prepared in the 'up' position is triggered by the black-body radiation field in the cavity, which gives to the system a small 'tipping angle' θ^i whose expectation value is (Moi *et al.* 1983)

$$\overline{\theta^i} = 2\left(\frac{1+k_{\mathrm{B}}\,T/h\nu}{N}\right)^{\frac{1}{2}}, \tag{10}$$

where T is the temperature of the thermal radiation in the cavity and k_{B} is the Boltzmann constant. (We assume $k_{\mathrm{B}}T/h\nu \gg 1$.)

If the cavity damping contribution in (8) is relatively small ($T_{\mathrm{cav}} \geqslant 10T_{\mathrm{r}}$; large Q or very large atom numbers N), (8) describes an oscillatory régime reminiscent of Rabi nutation: the atoms, strongly coupled to the cavity, oscillate back and forth between levels nl and $n'l'$, undergoing a self-nutation process induced by their own radiation field. If on the other hand the cavity damping term is large enough ($T_{\mathrm{cav}} < T_{\mathrm{r}}$), which corresponds to the experiments we have performed so far (T_{cav} is typically 10 ns and T_{r} is equal to 20 ns or more), the second-order derivative term in (8) can be neglected and the maser evolution is described by an 'over-damped' pendulum equation

$$\mathrm{d}\theta/\mathrm{d}t = (1/2T_{\mathrm{r}})\sin\theta, \tag{11}$$

which corresponds to a monotonic increase of θ from 0 to π, the atomic system being irreversibly damped by its own radiation field within a time of a few times T_{r}. More precisely, (11) with initial condition (10) is readily integrated to yield for the radiated energy in the cavity:

$$\left(\frac{\mathrm{d}\theta}{\mathrm{d}t}\right)^2 = \frac{1}{4T_{\mathrm{r}}^2}\frac{1}{\cosh^2\{(t-t_{\mathrm{d}})/2T_{\mathrm{r}}\}}, \tag{12}$$

with

$$t_d = -2T_r \lg \tfrac{1}{2}\theta^i = \frac{\hbar\epsilon_0 v}{2d^2 Q N} \lg\left(\frac{N}{1+k_B T/h\nu}\right). \quad (13)$$

Equation (12) describes a so-called hyperbolic secant pulse (represented in figure 8*b*) which reaches its maximum after an average delay t_d depending upon the atom number, the cavity Q and the thermal background temperature T (equation (13)).

It is interesting to notice that equations (11)–(13) are identical to those derived in the theory of optical superradiant emission of an ensemble of two-level atoms located in a volume small

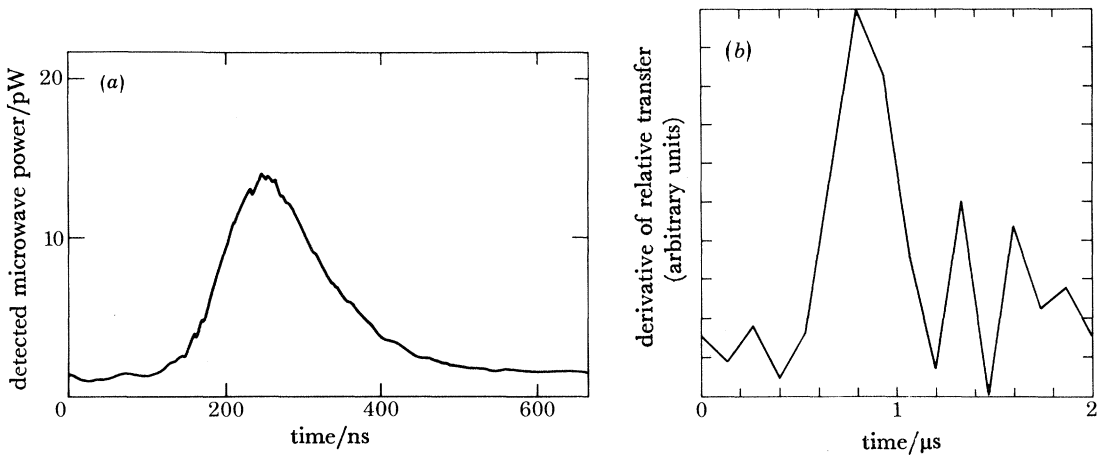

FIGURE 9. Examples of detected Rydberg maser pulses. (*a*) Maser emission on the 33S → 32P$_{\frac{1}{2}}$ transition in Na at $\nu = 108$ GHz. Direct heterodyne Schottky diode detection. $N = 200\,000$ atoms. (*b*) Maser emission on the 30S → 28P$_{\frac{1}{2}}$ transition in Na at $\nu = 457.5$ GHz, detected by field ionization. $N = 50\,000$ atoms.

compared with their emission wavelength λ and radiating spontaneously in free space (Dicke 1954), provided that in (13) we replace v/Q by $3\lambda^3/4\pi^2$ and set $T = 0$ K. This is not surprising because the situation we are studying here is in fact very similar to superradiance, the first difference being that the atoms in a transient Rydberg maser are 'superradiating' in the presence of their images in the cavity walls (which explains the replacement of λ^3 by a term proportional to v/Q), the other difference being that the fluctuations of the thermal radiation at room temperatre for millimetre-wave frequencies are more important than those of the vacuum field (which explains the $k_B T/h\nu$ factor in (3)). In other words, the transient Rydberg maser is a perfect model for Dicke superradiance and our experiments on these systems provide a very simple check of the Dicke theory.

Examples of radiation pulses exhibiting a bell-shaped time variation are shown in figures 9*a*, *b*. Figure 9*a* shows a maser emission signal on the 33S → 32P$_{\frac{1}{2}}$ transition in Na at $\nu = 108$ GHz, corresponding to approximately $N = 2 \times 10^5$ atoms. The emission (about 10 pW) is detected direct by the Schottky diode receiver. In figure 9*b*, the maser emission of $N \approx 50\,000$ atoms on the 30S → 28P$_{\frac{1}{2}}$ transition at $\nu = 457.5$ GHz is detected by the indirect radiation population transfer signal. The method is similar to that described in §4: the maser is 'frozen' after a variable delay Δt by the application of a small d.c. electric field and the time derivative of the population transfer from level 30S to level 28P$_{\frac{1}{2}}$ is plotted against Δt. Note the good agreement between the experimental pulse shape in this case and the theoretical hyperbolic secant shape (shown by the dashed line in figure 9*b*). The population transfer detection by the ionization of

Rydberg atoms appears to be more sensitive than the heterodyne method, the atoms themselves being used to detect their own radiation field: this is more efficient than an external detector, whose efficient coupling to the emitted field is more difficult to achieve. Furthermore, the time constant of the detection in the Rydberg ionization method is limited by the rise-time of the 'freezing' electric field, i.e. a few nanoseconds, which is much shorter than the 80 ns time constant of the heterodyne receiver. By a systematic study of such signals, we have checked the various predictions of the theory (Moi *et al.* 1983): pulse shapes, variation of the emission delay with atom number, electric dipole matrix element and temperature have been found to be in fair agreement with (12) and (14).

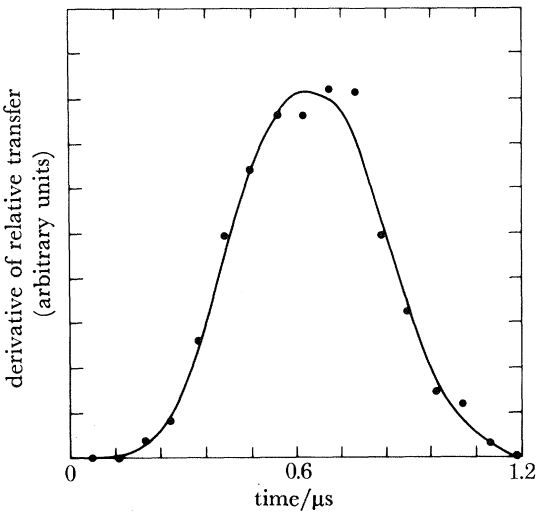

FIGURE 10. Very small maser signal on the 30S → 29P$_{\frac{1}{2}}$ transition detected by field ionization. $N = 1000$ atoms only.

A remarkable feature of these experiments – related to the property already mentioned in § 4 – is that maser emission can be observed with extremely low absolute atom numbers. For maser action to occur, the characteristic time T_r must be shorter than the drift time of the atom through the cavity (*ca.* 3 μs). Owing to the extremely large d, this condition is achieved with N as small as a few hundred, even for moderate cavity quality factors ($Q \approx 10^4$). This value is at least six orders of magnitude below the threshold that one usually observes for ordinary maser systems. In figure 10, we show as an illustration a very small maser signal observed on the 30S → 29P$_{\frac{1}{2}}$ transition in Na ($\nu = 140$ GHz). It corresponds to only $N = 10^3$ atoms. Maser action for N as small as 200 has been achieved at the present stage of the experiment.

6. Towards 'single-atom masers': resonant coupling of a Rydberg atom with a millimetre-wave cavity

By increasing the Q of our cavity ($Q \approx 10^6$ should be attainable by using superconducting mirrors), we hope to be able to realize even smaller maser systems. The ultimate limit would be to get a single atom interacting resonantly with the cavity. In that case, the classical description of § 5, valid for N large enough, no longer holds and one should shift to a full quantum-mechanical description. The situation that we have in mind is sketched in figure 11*a*: a single

two-level atom interacts with the harmonic oscillator-like mode of a resonant cavity. Initially, the atom is in the level + and the cavity empty (in the $n = 0$ level). Owing to atom-field interaction, the combined system initially in state $|+, 0\rangle$ is coupled to the state $|-, 1\rangle$ corresponding to the atom in the lower state, with one photon in the field. The coupling between these states results in a quantum mechanical oscillation between them, which is the Rabi nutation of a single atom in the field of a photon exchanged with the cavity (figure 11*b*). This field is simply expressed as

$$\mathscr{E}_{\text{single photon}} = (h\nu/2\epsilon_0 v)^{\frac{1}{2}}, \tag{14}$$

which for a $v = 0.01$ cm^3 cavity and a $\nu = 10^{11}$ Hz frequency is of the order of 4×10^{-4} V cm^{-1}, i.e. about one-tenth of the external field applied in the experiment of figure 6. We thus expect in this case a 200 kHz nutation (figure 11*b*) that could be observed if the transit time of the

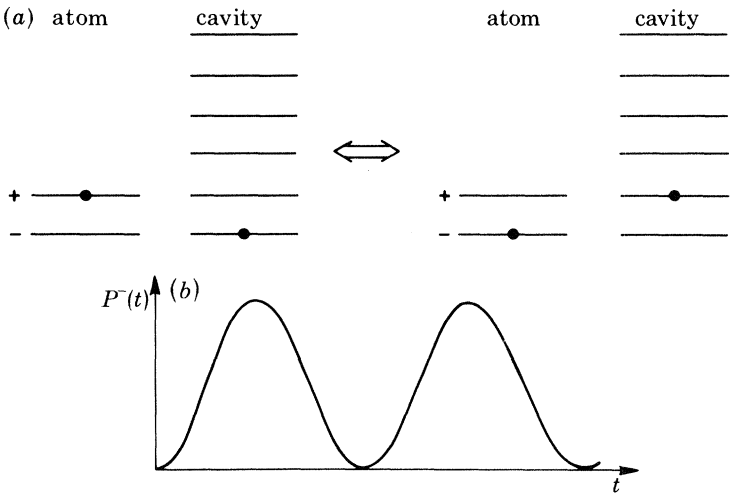

FIGURE 11. (*a*) Sketch of atomic and cavity energy levels for the single-atom maser experiment. (*b*) Predicted oscillation for the probability of finding the atom excited in the cavity: Rabi nutation of a single atom in the field of a single photon.

atom and the cavity damping time are made long enough (of course the expected nutation is damped with a time constant equal to T_{cav}). Such an experiment would thus require high-quality small cavities with a slow atomic motion through the mode waist. The detection procedure would be similar to that described above for Rabi nutation detection. Reducing the atom number to single atoms does not seem unrealistic and this single-atom–single-photon nutation experiment appears feasible. It would be a direct observation of the strong modification brought to spontaneous emission by the presence of cavity walls and the first experiment in which single photons would have been exhibited at such long wavelengths.

7. RYDBERG ATOMS AS DETECTORS OF MILLIMETRE-WAVE RADIATION

The above discussion has clearly emphasized the great sensitivity of Rydberg atoms to radiation at millimetre wavelengths. To conclude this review, we mention some experiments in which we have taken advantage of this sensitivity to detect very small amounts of radiation. Using our Rydberg masers as transient amplifiers, we have shown that it is indeed possible to amplify and measure small signals of the order of the black-body radiation background at the temperature of the atomic beam apparatus (Goy *et al.* 1983). The present sensitivity figure

PHILOSOPHICAL TRANSACTIONS OF THE ROYAL SOCIETY A MATHEMATICAL, PHYSICAL & ENGINEERING SCIENCES

(3×10^{-17} W Hz$^{-\frac{1}{2}}$ at room temperature) is remarkable for detectors in this frequency range. It will certainly be improved further when the system is operated, as planned, at 4 K. We have also used a beam of Rydberg atoms as a radiation 'absorber' to count the average number $n = \{\exp(h\nu/k_B T) - 1\}^{-1}$ of black-body photons stored in a single mode of the resonant cavity. The atoms are then prepared in the lower state of the transition resonant with the cavity mode and we count the number ΔN of atoms absorbing the black-body radiation field during the interaction time Δt. We have shown that this number tends towards the limit $\overline{\Delta N_{\text{lim}}} = 2\bar{n}$ for Δt long enough and we have interpreted this limit as resulting from a thermalization between the field mode and the atomic system (Raimond *et al.* 1982). (The observed limit is $2\bar{n}$ and not $\bar{n}$ because of atomic transition degeneracy.) Counting $\overline{\Delta N_{\text{lim}}}$ thus amounts to measuring the absolute radiation temperature T. This experiment can be seen as a counterpart of the Rydberg maser experiment: instead of starting from its 'up' position, the Bloch vector is initially in the 'down' direction (see figure 8*a*). It is 'kicked' away from this stable equilibrium state by the black-body field fluctuations, and the motion of the Bloch vector tip around $\theta = \pi$ can be analysed as a Brownian motion, with an average energy $2k_B T$, corresponding to $\overline{\Delta N} = 2k_B T/h\nu$ absorbed photons. In this experiment, the large electric dipole matrix element of the Rydberg atoms is again essential. For ordinary atoms, the thermalization time with black-body radiation is extremely long and this Brownian motion of the atomic polarization would be impossible to observe. Clearly these preliminary experiments show that Rydberg atoms can be used to perform photon counting and photon statistics experiments in the millimetre-wave domain, which opens the way to many interesting applications.

References

Abragam, A. 1961 *Principles of nuclear magnetism.* Oxford University Press.

Dicke, R. H. 1954 *Phys. Rev.* **93**, 99.

Evenson, K. M., Petersen, F. R. & Wells, J. S. 1974 In *Laser spectroscopy* (ed. R. G. Brewer & A. Mooradian), p. 143. New York: Plenum Press.

Fabre, C., Haroche, S. & Goy, P. 1978 *Phys. Rev.* A**18**, 229.

Fabre, C., Haroche, S. & Goy, P. 1980 *Phys. Rev.* A**22**, 778.

Goy, P., Moi, L., Gross, M., Raimond, J. M., Fabre, C. & Haroche, S. 1983 *Phys. Rev.* A. (In the press.)

Goy, P., Raimond, J. M., Vitrant, G. & Haroche, S. 1982 *Phys. Rev.* A. (In the press.)

Gross, M., Goy, P., Fabre, C., Haroche, S. & Raimond, J. M. 1979 *Phys. Rev. Lett.* **43**, 343.

Grynberg, G. & Cagnac, B. 1977 *Rep. Prog. Phys.* **40**, 791.

Moi, L., Fabre, C., Goy, P., Gross, M., Haroche, S., Encrenaz, P., Beaudin, G. & Lazareff, B. 1980 *Optics Commun.* **33**, 47.

Moi, L., Goy, P., Gross, M., Raimond, J. M., Fabre, C. & Haroche, S. 1983 *Phys. Rev.* A (In the press.)

Raimond, J. M., Goy, P., Gross, M., Fabre, C. & Haroche, S. 1982 *Phys. Rev. Lett.* **49**, 117.

PHILOSOPHICAL TRANSACTIONS OF THE ROYAL SOCIETY A MATHEMATICAL, PHYSICAL & ENGINEERING SCIENCES